Michael Hoffmann, Milan Pešić, Stefan Slesazeck, Uwe Schroeder, Thomas Mikolajick

On the stabilization of ferroelectric negative capacitance in nanoscale devices

Erstveröffentlichung in / First published in:

Nanoscale. 2018, 10(23), S. 10891-10899 {Zugriff am: 12.10.2022}. RSC. ISSN 2040-3372.

DOI: https://doi.org/10.1039/C8NR02752H

Final edited form was published in "Nanoscale". 2018, 10(23), S. 10891-10899. ISSN 2040-3372.
https://doi.org/10.1039/C8NR02752H

On the stabilization of ferroelectric negative capacitance in nanoscale devices†

Michael Hoffmann,*[a] Milan Pešić,[a] Stefan Slesazeck,[a] Uwe Schroeder,[a] Thomas Mikolajick [a,b]

Recently, the proposal to use voltage amplification from ferroelectric negative capacitance (NC) to reduce the power dissipation in nanoelectronic devices has attracted significant attention. Homogeneous Landau theory predicts, that by connecting a ferroelectric in series with a dielectric capacitor, a hysteresis-free NC state can be stabilized in the ferroelectric below a critical film thickness. However, there is a strong discrepancy between experimental results and the current theory. Here, we present a comprehensive revision of the theory of NC stabilization with respect to scaling of material and device dimensions based on multi-domain Ginzburg–Landau theory. It is shown that the use of a metal layer in between the ferro-electric and the dielectric will inherently destabilize NC due to domain formation. However, even without this metal layer, domain formation can reduce the critical ferroelectric thickness considerably, limiting not only the range of NC stabilization, but also the maximum amplification attainable. To overcome these obstacles, the downscaling of lateral device dimensions is proposed as a way to prevent domain formation and to enhance the voltage amplification due to NC. These insights will be crucial for future NC device design and scaling towards nanoscale dimensions.

1. Introduction

The future scaling of nanoscale transistor device dimensions is facing serious challenges due to power density constraints.[1] Currently, the power density is mostly limited by the supply voltage, which depends on the subthreshold swing S of the transistor, where S describes how much voltage is needed to change the current flowing through the device by one order of magnitude. However, because of the thermionic Boltzmann limit of $S \geq \ln(10)k_BT/q$, the supply voltage cannot be reduced much further. Here, k_B is the Boltzmann constant, T is the absolute temperature and q is the elementary charge. Therefore, either performance or off-state power consumption will degrade strongly in ultimately scaled devices.[2] To overcome this fundamental limit, the use of ferroelectric negative capacitance (NC) was proposed by Salahuddin and Datta in 2008.[3] This idea is based on homogeneous Landau theory and suggests that a ferroelectric material used as a gate insulator in a transistor could be stabilized in an NC state below a critical ferroelectric film thickness. In this NC state, the ferroelectric hysteresis should vanish and the transistor surface potential would be amplified with respect to the applied gate voltage, thus achieving a higher current with lower applied voltage.[3]

Since this first publication, many experimental investigations have shown that a variety of ferroelectric NC effects indeed exist.[4–10] However, these effects seem much more subtle than homogeneous Landau theory initially suggested.[11,12] From over half a century of research on ferroelectric materials, it is well-known that depolarization fields will cause the formation of domains in the ferroelectric to reduce the depolarization energy.[13–19] This is especially interesting, since depolarization fields are the stabilization mechanism of NC based on homogeneous Landau theory.[12] Nevertheless, only a small fraction of publications on NC has considered domain formation,[11,12,20,21] which is known to have a strong impact on the dielectric properties of ferroelectric materials and especially thin films.[22–24] Indeed, it has been already established, that domain wall motion itself can contribute negatively to the permittivity of a ferroelectric.[12,22,25,26] While we will not investigate NC from domain wall motion in this work, we will focus on the possibility of a stabilized NC state where the polarization completely vanishes as proposed by Salahuddin and Datta.[3] Nevertheless, since domains could still form, the use of homogeneous single-

[a]NaMLab gGmbH, Noethnitzer Str. 64, D 01187 Dresden, Germany.
E mail: michael.hoffmann@namlab.com

[b]Chair of Nanoelectronic Materials, TU Dresden, D 01062 Dresden, Germany

† Electronic supplementary information (ESI) available: Simulation methods for domain formation in the MFMIM and MFIM structures. The onset of domain formation in the MFIM structure as a function of the dielectric thickness is shown. Estimations and material constants for different ferroelectric materials are summarized. A derivation of eqn (2) is given. See DOI: 10.1039/C8NR02752H

Final edited form was published in "Nanoscale". 2018, 10(23), S. 10891-10899. ISSN 2040-3372.
https://doi.org/10.1039/C8NR02752H

domain Landau theory to model such NC effects is not suitable and will lead to wrong predictions and NC device design as will be shown in this work. Therefore, we will apply Ginzburg–Landau theory to model NC stabilization, which considers the energy of polarization gradients.

While many reported NC devices show a hysteretic behavior which is characteristic for ferroelectric materials, these NC effects are obviously not stabilized and only transient in nature.[7–10] Here, to avoid confusion, we want to make a clear distinction between these *transient* NC effects in ferroelectrics, which are hysteretic, and *stabilized* NC without any hysteresis. Especially in publications in the device engineering community, this critical distinction is rarely made.[27,28] It should also be mentioned that the directly measurable small-signal capacitance of any capacitor will always be positive, which means that stabilized NC can only be observed indirectly.[29,30] While the use of transient NC from ferroelectric switching might be too slow for digital applications,[27] it was recently found that stabilized NC should be fast enough.[31] Further adding to the confusion surrounding the topic, in the literature there are in principle two different structures which were proposed to stabilize NC, which are shown in Fig. 1: a metal–ferroelectric–metal–insulator–metal (MFMIM)[32–36] and a metal–ferroelectric–insulator–metal (MFIM) structure.[3,4,12,37] Similar MFIM heterostructure or superlattice capacitors are also of interest for many fundamental studies on ferroelectricity.[38,39] While we will only discuss capacitor structures with a bottom metal electrode here for simplicity, the basic physics of NC stabilization will be the same when the bottom metal is replaced by a semiconductor channel as in an NC field-effect transistor (MFMIS *vs.* MFIS). The MFMIS structure is often reported in literature since it is experimentally very easy to connect existing MFM capacitors to the gate of regular transistors, while also being able to measure both components individually.

The goal of this work is to reconcile the well-known theory of ferroelectric domain formation caused by depolarization fields with the theory of NC stabilization in nanoscale devices. We hope that this will help to clear up some of the confusion surrounding the topic and act as a guideline for further experimental and theoretical work on ferroelectric NC. The paper is organized as follows: first, we will introduce the Landau free energy expressions for the dielectric and for the ferroelectric when allowing domain formation and considering the electrostatic self-energy term. Consequently, we will look at the special case of homogeneous polarization, which is identical for the MFMIM and MFIM structure, and introduce new NC stabilization conditions caused by the self-energy. Afterwards, the effects of domain formation are discussed first for the MFMIM and then for the MFIM structure, with a focus on the scaling of device dimensions. Finally, the main results will be summarized and important conclusions for NC devices will be drawn.

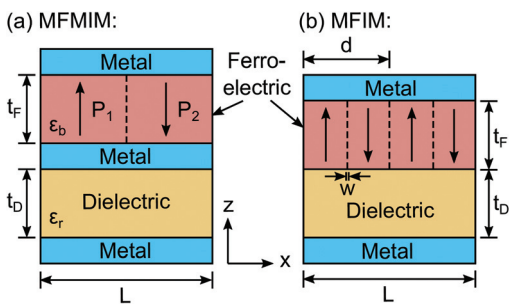

Fig. 1 Two different suggested structures for stabilization of NC: (a) MFMIM and (b) MFIM stack. Dashed lines indicate domain walls with width *w*. Arrows indicate polarization directions.

2. Results and discussion

2.1. Multi-domain Landau free energy potentials

To revise the theory of NC stabilization, we will introduce two physical effects which have not been considered in detail before: domain wall energy caused by domain formation and electrostatic self-energy of the ferroelectric. While domain formation is usually described by Ginzburg–Landau theory, the self-energy was shown to be critical even in homogeneous Landau theory, especially when describing nanoscale ferroelectrics.[40] Considering these effects, the Helmholtz free energy density per unit volume (which we will just call "free energy" from here on) of the ferroelectric can be written as

$$u_F = \alpha P^2 + \beta P^4 + \gamma P^6 + k(\nabla P)^2 + \frac{\varepsilon_0 \varepsilon_b}{2} {E_F}^2, \qquad (1)$$

where α, β and γ are the ferroelectric anisotropy constants, P is the spontaneous electric polarization, k is the domain wall coupling constant and E_F is the electric field in the ferroelectric. The electric displacement field is then defined as $D_F = \varepsilon_0 \varepsilon_b E_F + P$, where ε_0 and ε_b are the vacuum permittivity and relative background permittivity of the ferroelectric, respectively. Notice that P is only the spontaneous part of the polarization and that the total polarization in the ferroelectric is given by $P_T = P + \varepsilon_0(\varepsilon_b - 1)E_F$.[40] By setting $k = 0$ and $\varepsilon_b = 0$ in eqn (1), one obtains the same homogeneous Landau free energy density without electrostatic self-energy which has been used in most publications on NC so far.[3]

While we will not assume $k = 0$ and $\varepsilon_b = 0$ here, a few simplifying assumptions to eqn (1) are useful in order to present the results as clear as possible without changing the basic physics: it is assumed that the spontaneous polarization P of the ferroelectric is only oriented perpendicular to the film plane in the *z*-direction as defined in Fig. 1. Furthermore, we will consider the formation of two domains of equal size with polarization P_1 and P_2, which can be extended to an infinite film by using periodic boundary conditions. The domain wall width w is assumed to be constant and much smaller compared to the domain period d, see Fig. 1. For simplicity, we only consider domain formation in the *x*-direction. Further, we will neglect the higher order γP^6 term and assume that the ferroelectric exhibits a second-order phase transition with $\alpha < 0$ and $\beta > 0$. Using these assumptions for a finite film of lateral dimension

Final edited form was published in "Nanoscale". 2018, 10(23), S. 10891-10899. ISSN 2040-3372.
https://doi.org/10.1039/C8NR02752H

L, we can write down the free energy per volume of the whole ferroelectric as

$$u_F = \frac{\alpha}{2}\left(P_1^2 + P_2^2\right) + \frac{\beta}{2}\left(P_1^4 + P_2^4\right) + \left(\frac{2}{d} \quad \frac{1}{L}\right)\frac{k}{w}(P_1 \quad P_2)^2 + \frac{\varepsilon_0\varepsilon_b}{2}E_F^2. \tag{2}$$

First, we will look at u_F in eqn (2) as a function of the polarization of both domains P_1 and P_2 when $k = 0$ and $E_F = 0$. The detailed derivation of eqn (2) and used simulation parameters are given in the section S1 of the ESI.† From the depiction in Fig. 2, it is apparent that there are four degenerate energy minima corresponding to both domains switched up (↑↑), both switched down (↓↓) and two anti-parallel alignments of P_1 and P_2 (↑↓ or ↓↑). For $P_{1,2} \approx 0$ there is an energy barrier which coincides with the NC region of the ferroelectric. The ferroelectric has to be stabilized at this point in order to utilize NC for hysteresis-free device operation. Furthermore, it can be observed that this barrier height is significantly reduced between neighboring energy minima, *e.g.* (↑↑) and (↑↓) or (↑↓) and (↓↓). This intuitively shows, that when the ferroelectric switches, from (↑↑) to (↓↓), the polarization will switch through intermediate domain states (↑↓) or (↓↑), because the barriers for these processes are much smaller compared to the one at $P_{1,2} \approx 0$. Here, we want to note that the NC state does not only exist when P is exactly zero, but also for finite polarization values in the vicinity of $P = 0$. That means, in the stabilized NC state, when an external field is applied (which is small compared to the coercive field), the ferroelectric will have non-zero P, but still be in an NC state and go back to $P = 0$ when the external field is removed.

Similarly to eqn (1), we can now also construct a free energy density u_D for the dielectric material shown in Fig. 1. Under the assumption of a linear and isotropic dielectric with relative permittivity ε_r, we can write

$$u_D = \frac{\varepsilon_0\varepsilon_r}{2}E_D^2, \tag{3}$$

where E_D is the electric field in the dielectric and the electric displacement field is defined as $D_D = \partial u_D/\partial E_D = \varepsilon_0\varepsilon_r E_D$. Furthermore, the permittivity of the dielectric can be obtained from $(\partial^2 u_D/\partial D_D^2)^{-1} = \varepsilon_0\varepsilon_r$, which confirms the consistency of eqn (3). Both eqn (2) and (3) will form the basis of the following discussions on the stabilization of NC. To completely assess the stability of the NC state at $P_{1,2} \approx 0$ in Fig. 2, it is sufficient to investigate the two orthogonal cases in the (P_1,P_2)-plane: (I) the single-domain case ($P_1 = P_2$) and (II) the anti-parallel domain case ($P_1 = -P_2$). First, we will revisit the homogeneous single-domain case (I).

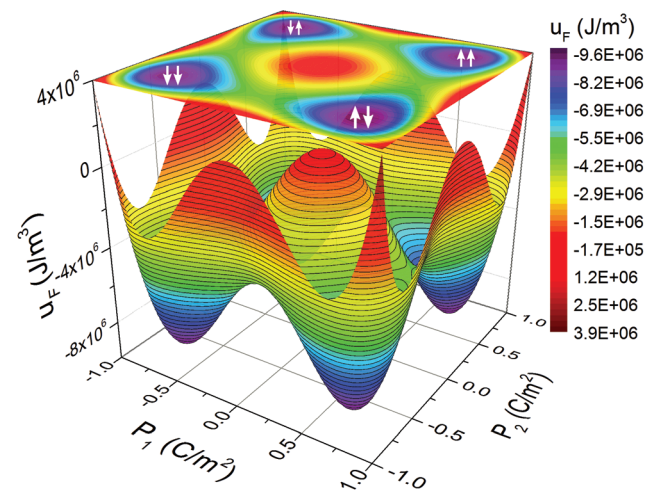

Fig. 2 Free energy of a ferroelectric with two equally sized domains as a function of the polarization of two domains of equal size P_1 and P_2. Arrows indicate polarization directions.

2.2. Single-domain case

Initially, it should be noted that in the single-domain case, the electrostatics in the MFMIM and MFIM structure are completely equal when leakage currents through the layers are neglected, as done here. The implications of leakage in both structures have been discussed elsewhere, where it has been shown that in the MFMIM case, leakage will destabilize NC in the DC limit.[41] Furthermore, in the single-domain case, the electrostatics can be completely solved in one dimension, which is the z-direction of the spontaneous polarization. With the electrical boundary conditions

$$\varepsilon_0\varepsilon_r E_D = \varepsilon_0\varepsilon_b E_F + P, \quad V = t_F E_F + t_D E_D, \tag{4}$$

where t_D is the thickness of the dielectric and V the potential difference between the top and bottom electrode, we can then calculate E_F and E_D as a function of P as

$$E_F = \frac{1}{t_F C_0}(\quad P + C_D V), \quad E_D = \frac{1}{t_D C_0}(P + C_{Fb}V). \tag{5}$$

Here the capacitance per unit area C_0 is conveniently defined as

$$C_0 = \varepsilon_0\left(\frac{\varepsilon_r}{t_D} + \frac{\varepsilon_b}{t_F}\right) = C_D + C_{Fb}, \tag{6}$$

where C_D and C_{Fb} are the dielectric capacitance per area and ferroelectric background capacitance per area, respectively. Since we are interested in the stability of NC under equilibrium conditions, we will set $V = 0$ (short circuit condition). However, when a relatively large voltage (compared to the coercive voltage) would be applied, the ferroelectric might temporarily be in a positive capacitance state, but when the voltage is removed again, it would return to the stabilized NC state, which we investigate here. For $P_1 = P_2 = P$ and using eqn (2) and (5) the ferroelectric free energy then yields

$$u_F = \left(\alpha + \frac{C_{Fb}}{2t_F C_0^2}\right)P^2 + \beta P^4. \tag{7}$$

Final edited form was published in "Nanoscale". 2018, 10(23), S. 10891-10899. ISSN 2040-3372.
https://doi.org/10.1039/C8NR02752H

Analogously, utilizing eqn (3) and (5), we can then obtain the free energy density of the dielectric as

$$u_D = \frac{C_D}{2t_D{C_0}^2}P^2. \quad (8)$$

Finally, using eqn (7) and (8), we can now calculate the total free energy density per unit area of the system as $U_T = u_F t_F + u_D t_D$, which yields

$$U_T = \left(\alpha t_F + \frac{1}{2C_0}\right)P^2 + \beta t_F P^4. \quad (9)$$

Eqn (9) gives us the stability condition for the total system in the single-domain case: for the system to be stable at $P = 0$, the second derivative $\partial^2 U_T/\partial P^2$ has to be larger than zero, which means that $2\alpha t_F + 1/C_0$ also has to be positive. The P^4 term can be neglected for $P \approx 0$. Rearranging this condition we can calculate a maximum critical thickness of the ferroelectric, for which this is the case:

$$t_F < t_{F,\max} = \frac{1}{2\alpha C_D}(1 + 2\varepsilon_0\varepsilon_b\alpha). \quad (10)$$

The first term in eqn (10) is exactly the same result which was first calculated by Salahuddin and Datta.[3] However, there is a correction to this condition due to the fact that $\varepsilon_b \neq 0$, which was neglected in the original publication. It should be noted that the condition in eqn (10) was also obtained by Bratkovsky and Levanyuk when considering the effect of dead layers and non-ideal electrode interfaces.[42] Furthermore, we can see from eqn (10), that for $t_{F,\max} > 0$, we have another condition to satisfy, which is

$$\varepsilon_b\alpha > -\frac{1}{2\varepsilon_0}. \quad (11)$$

This result is surprising and demands reconsideration of not only α as the decisive material parameter for NC stabilization, but also ε_b. In general in the single-domain case, t_F should be designed as close as possible to, but not larger than, $t_{F,\max}$ to obtain the maximum capacitance enhancement or voltage amplification without hysteresis. For $t_F > t_{F,\max}$, only transient NC might be observed during switching, which will be accompanied by a hysteresis.[10]

2.3. Multi-domain case

We have now defined the NC stabilization condition for the single-domain case. Nevertheless, to completely assess the NC stability of the system in Fig. 2, we also have to investigate the anti-parallel multi-domain case $P_1 = -P_2$. However, the electrical boundary conditions for the MFMIM and MFIM structures as shown in Fig. 1 are now different and therefore have to be considered separately. We will start with the MFMIM structure, since in this case all the electrostatics can be again solved in the z-direction only.

2.3.1. Metal–ferroelectric–metal–insulator–metal (MFMIM) structure. In the MFMIM structure, when assuming ideal ferroelectric/metal interfaces, the electrical boundary conditions for a ferroelectric with two domains are identical to eqn (4) and (5) when we substitute $P = (P_1 + P_2)/2$. This immediately tells us that for $V = 0$ and $P_1 = -P_2$, the depolarization field in the ferroelectric E_F completely vanishes. This additionally results in $E_D = 0$ and thus $u_D = 0$, independent of P_1 and P_2. If we now again write down the total energy density per area U_T for $P_1 = -P_2 = P$, which is then identical to $t_F u_F$, we will see the implications on NC stabilization:

$$U_T = t_F\left[\alpha + \left(\frac{2}{d} \quad \frac{1}{L}\right)\frac{4k}{w}\right]P^2 + t_F\beta P^4. \quad (12)$$

Notice that eqn (12) is completely independent of ε_r, ε_b and t_D, because E_F and E_D are zero. This shows that the only means to prevent anti-parallel domain formation in an MFMIM structure is an increase of the domain wall energy term $4k(2/d - 1/L)/w$. Since we know that $E_F = 0$ for $P_1 = -P_2$ in an ideal MFMIM structure, exactly two domains will form, because this case corresponds to the lowest overall energy of the system. While an increase in the (even) number of domains $2L/d$ would also lead to $E_F = 0$, the domain wall energy would increase with $1/d$, as seen in eqn (12). Therefore, in the MFMIM case we can set $d = L$ which has the lowest overall free energy. We then obtain the following condition for the stability at $P = 0$ in eqn (12):

$$\alpha + \frac{4k}{wL} > 0. \quad (13)$$

This means, that we can then define, in addition to $t_{F,\max}$, a maximum critical *lateral* dimension L_{crit}, which is can be expressed as

$$L < L_{crit} = -\frac{4k}{\alpha w}. \quad (14)$$

Eqn (14) shows that to stabilize NC in an MFMIM structure, all lateral device dimensions have to be so small that the domain wall energy becomes large enough to prevent the formation of anti-parallel domains. In this case, the ferroelectric would behave exactly as predicted in homogeneous Landau theory and NC could be stabilized. However, far from the transition temperature of the ferroelectric, L_{crit} should be in the order of ~1 nm, which is much smaller than any practical device could be. Calculations of L_{crit} for typical ferroelectric materials can be found in the ESI.† How this stabilization of NC through domain wall energy works, can be seen from the $U_T(P_1,P_2)$ energy landscapes in Fig. 3, where $t_F < t_{F,\max}$ is always fulfilled. Simulation parameters can be found in section S1 of the ESI.†

In the first case of $L \gg L_{crit}$, which is shown in Fig. 3(a), we can see that the two energy minima for homogeneous polarization (↑↑) and (↓↓), have vanished completely. This is due to the depolarization energy of the dielectric as discussed for the single-domain case before. However, both energy minima for anti-parallel domains (↑↓) and (↓↑) are unaffected compared to Fig. 2, since the domain wall energy reduces to zero in the limit of $L \to \infty$. Therefore, NC cannot be stabilized at $P_{1,2} = 0$, since this point is actually a saddle point and not an energy minimum of the system as suggested by homogeneous Landau

Final edited form was published in "Nanoscale". 2018, 10(23), S. 10891-10899. ISSN 2040-3372.
https://doi.org/10.1039/C8NR02752H

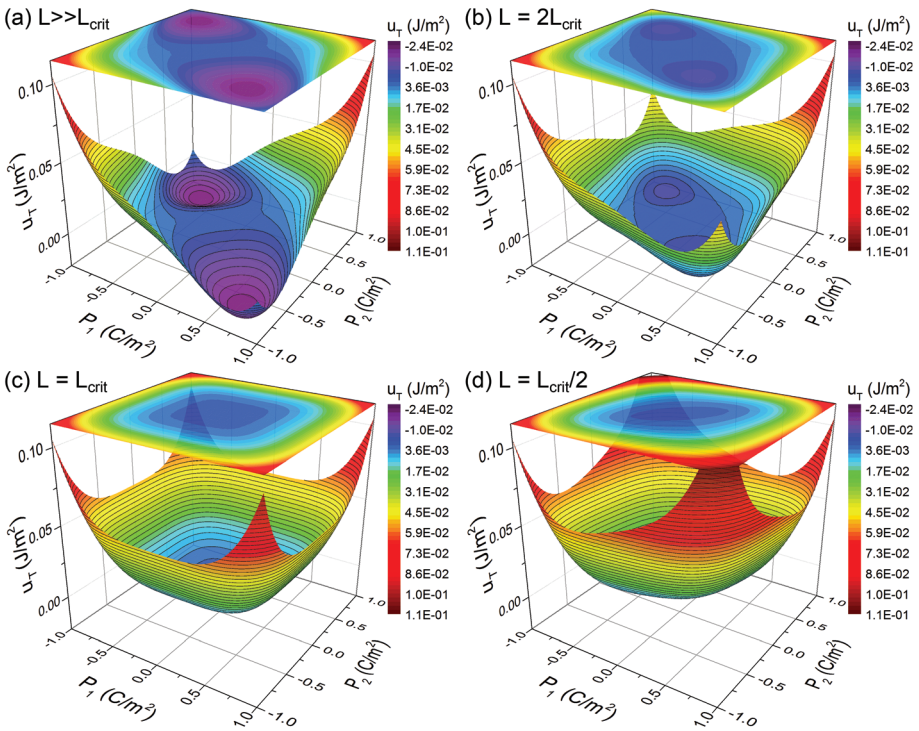

Fig. 3 Total free energy density per area of a MFMIM structure with different lateral dimensions (a) $L \gg L_{crit}$, (b) $L = 2L_{crit}$, (c) $L = L_{crit}$ and (d) $L = L_{crit}/2$ as a function of the domain polarizations P_1 and P_2.

theory.[20] This means that even the smallest perturbation of the ferroelectric in the state $P_{1,2} = 0$ will lead to a spinodal decomposition into a multi-domain state. The same is true for the second case, where $L = 2L_{crit}$ in Fig. 3(b). Here, we can see that the domain wall energy increases, however not sufficiently to eliminate the energy minima of the anti-parallel domain configurations. When $L = L_{crit}$ on the other hand, which is shown in Fig. 3(c), there is only one energy minimum at $P_{1,2} = 0$, since the domain wall energy is now large enough to prevent domain formation and the depolarization energy of the dielectric stabilizes the NC state. Finally, in the case where $L < L_{crit}$ in Fig. 3(d), the system remains stabilized at the $P_{1,2} = 0$ energy minimum. While the energy curvature along the $P_1 = -P_2$ axis is increased compared to the $L = L_{crit}$ case, the curvature along the $P_1 = P_2$ axis, which is inversely proportional to the total capacitance C_T, is unaffected.[43] Therefore, the capacitance enhancement due to NC should be independent of L for $L \leq L_{crit}$.

What this shows is that using an MFMIM structure is generally unfavorable for NC devices, since it imposes very strict limits for lateral device dimensions in the range of nanometers. Therefore, large area MFMIM devices cannot exhibit stabilized NC as long as anti-parallel domains can form. Furthermore, having a floating metal gate in such a nanoscale device will inevitably be prone to charging effects due to leakage currents which also would impede reliable operation.

2.3.2. Metal–ferroelectric–insulator–metal (MFIM) structure. To investigate domain formation in the MFIM structure, 2D electrostatics have to be solved, since the boundary condition at the ferroelectric/dielectric interface is discontinuous when $P_1 = -P_2$. The electrostatics of the MFIM structure in Fig. 1(b) are solved numerically using an iterative Poisson solver for different geometries and material properties, which is described in detail in section S2 of the ESI.† First, we assume an infinite film in x-direction ($L \to \infty$) and use periodic boundary conditions at the edges of the domains to calculate the equilibrium domain period d_{eq}. To do this, different domain periods d are simulated and the total free energy of the system per domain period U_T is calculated as a function of d. Note that U_T per domain period is identical to the total energy density of the system if the MFIM structure has infinite lateral dimensions and is periodic in x-direction. Fig. 4 shows U_T as a function of the domain period d and the magnitude of the anti-parallel polarization $P_1 = -P_2$ for two different thicknesses t_F. For NC to be stable in this structure, we again need an energy minimum at $P_1 = -P_2 = 0$, but now for all possible domain periods d. As can be seen in Fig. 4(a), this condition is not fulfilled, since there are two degenerate energy minima at $P_{1,2} \neq 0$, which correspond to the multi-domain state. These minima define the equilibrium domain period d_{eq}. For $d > d_{eq}$ the depolarization energy dominates the total free energy U_T, stabilizing the $P_{1,2} = 0$ state only for larger domain periods. On the other hand, for $d < d_{eq}$, U_T is dominated by the domain wall energy, which is also able to stabilize the $P_{1,2} = 0$ state when d is small enough. However, since d is not fixed in an infinite film, the ferroelectric will always relax to the multi-

Final edited form was published in "Nanoscale". 2018, 10(23), S. 10891-10899. ISSN 2040-3372.
https://doi.org/10.1039/C8NR02752H

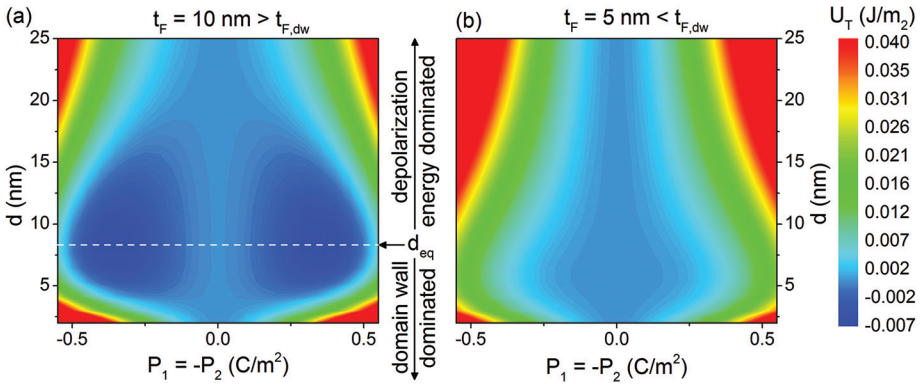

Fig. 4 Total free energy of an infinite MFIM structure with anti parallel domains as a function of the domain period d and the polarization (a) for $t_F > t_{F,dw}$ and (b) $t_F < t_{F,dw}$.

domain state at $d = d_{eq}$ in the case of Fig. 4(a). It should be noted, that $t_F < t_{F,max}$ is valid in all of these simulations, which means that the knowledge of $t_{F,max}$ is not sufficient to determine the stability of the NC state in the MFIM structure.

Nevertheless, when performing the same simulation for an even smaller thickness t_F, as shown in Fig. 4(b), we observe that the multi-domain energy minima vanish and only a single minimum at $P_{1,2} = 0$ is visible for all domain periods d. This shows, that there is indeed a critical thickness $t_{F,dw}$ below which no anti-parallel domains will form, but also that it is completely different from $t_{F,max}$ in eqn (10). Our simulations show that for $t_F < t_{F,dw}$, the sum of the domain wall energy and depolarization energy for any polarization $P_1 = -P_2 \neq 0$ is larger than the negative contribution of the ferroelectric anisotropy energy which is given by the first two terms on the right hand side of eqn (2). Because of this, the $P_1 = -P_2 = 0$ state is energetically more favorable compared to any other configuration with finite polarization.

To determine an analytic formula for $t_{F,dw}$, we simulated different MFIM structures while varying the parameters, k/w, α, ε_b, ε_r and t_D. In the end we obtain the empirical equation

$$t_F < t_{F,dw} \approx \frac{2k}{\alpha^2 \varepsilon_0 (\varepsilon_b + \varepsilon_r) w}, \quad (15)$$

for which no domains will form in an infinite film. We can see from eqn (15) that $t_{F,dw}$ is proportional to the domain wall coupling term k/w and inversely proportional to the permittivities of both layers as well as α^2. This differs significantly from the formulas for the critical thickness used in the literature so far. The only somewhat similar result was obtained by Cano and Jiménez when considering the suppression of sinusoidal domain patterns when stabilizing NC.[11] Furthermore, eqn (15) does not depend on the thickness of the dielectric layer t_D at all, if t_D is large enough (roughly larger than $d_{eq}/2$).[12,44] In this case the electric field lines in the dielectric will be able to close completely and the rest of the dielectric will be almost field-free. Obviously, this is only the case when no external voltage is applied to the MFIM structure. However, if t_D is smaller than $d_{eq}/2$, the polarization will interact with the bottom electrode and therefore will reduce $t_{F,dw}$ abruptly. This is shown in Fig. S1 of the ESI.†

There are some important implications of the behavior in Fig. S1† for NC device design. First, for NC stabilization, C_D is not the critical design parameter, but only ε_r, because for the ferroelectric it is only important what happens in a certain region in the dielectric of about $d_{eq}/2$ from the ferroelectric/dielectric interface. Secondly, in an MFIS structure, where the insulator is a very thin SiO_2 layer on top of a Si substrate, in inversion the stack can be thought of as an MFIM structure with very small t_D. Therefore, looking at Fig. S1,† NC might not be stable in the whole operating range of the transistor, but only in the subthreshold regime.

Now, in analogy to the discussion of the MFMIM structure, we will investigate how a finite lateral film dimension L will affect domain formation and therefore, NC stability. For MFIM structures where $L \gg d_{eq}$, no significant deviation from eqn (15) is expected, since d_{eq} will not differ substantially from the infinite film case. However, when L becomes similar to or even smaller than d_{eq} in the infinite film case, considerable changes in the energy densities are expected. Since $L = nd$ in a finite MFIM structure with an anti-parallel domain configuration, where n is a positive integer, d will always be equal to or smaller than L in this case. Thus, reducing L below d_{eq} (infinite film case), will reduce d accordingly. As we can see from eqn (3) and Fig. 4, in this regime ($L < d_{eq}$) the domain wall energy density is proportional to $1/L$ and will dominate the total energy of the system. A reduction of $L < d_{eq}$ of the MFIM stack could then increase the domain wall energy density considerably, thus destabilizing the anti-parallel domain state. Therefore, it should be possible to effectively increase $t_{F,dw}$ by decreasing L below d_{eq}. In this case, $t_{F,dw}$ should increase proportional to $1/L$ (since it is proportional to the domain wall energy density, $t_{F,dw} \sim k/w$), thus allowing a higher amplification compared to a film with $L \to \infty$. Nevertheless, infinite amplification as expected from single-domain theory would still be impossible, since L would again have to be in the range of L_{crit}, which is too small for practical devices. In general, it

Final edited form was published in "Nanoscale". 2018, 10(23), S. 10891-10899. ISSN 2040-3372.
https://doi.org/10.1039/C8NR02752H

can be expected that $t_{F,dw}$ is significantly smaller than $t_{F,max}$, which will reduce the NC stabilization window. How this would look like is sketched in Fig. 5(b) in comparison to an MFMIM structure in 5(a).

These graphs show the voltage amplification $A = C_T/C_D$, as a function of t_F and L. Striped regions indicate a multi-domain configuration under the presence of depolarization fields. In the MFMIM case, hysteresis can only be avoided if $t_F < t_{F,max}$ and $L < L_{crit}$. In the MFIM case on the other hand, the hysteresis will vanish for $t_F < t_{F,dw}$, even when $L \to \infty$. Another important difference between the MFMIM and the MFIM case is, that in the latter, even a multi-domain configuration can result in small-signal NC, as was shown by Zubko *et al.*[12] However, the boundary conditions for this multi-domain NC stabilization are still not clear and have to be investigated in the future. Nevertheless, this does not change the fact that in the MFMIM case, a multi-domain configuration will always lead to hysteresis. While first-principles calculations have shown that in $BaTiO_3/SrTiO_3$ capacitors, even two unit cell wide domains can form,[45] it is not yet clear if such behavior is expected in the newly discovered HfO_2 and ZrO_2 based ferroelectrics, which are most promising for NC devices.[46] If domain formation in these materials cannot be prevented by scaling of the lateral device dimensions as suggested here, stabilized NC might still emerge in certain multi-domain configurations, which are a promising topic for future studies on ferroelectric NC.

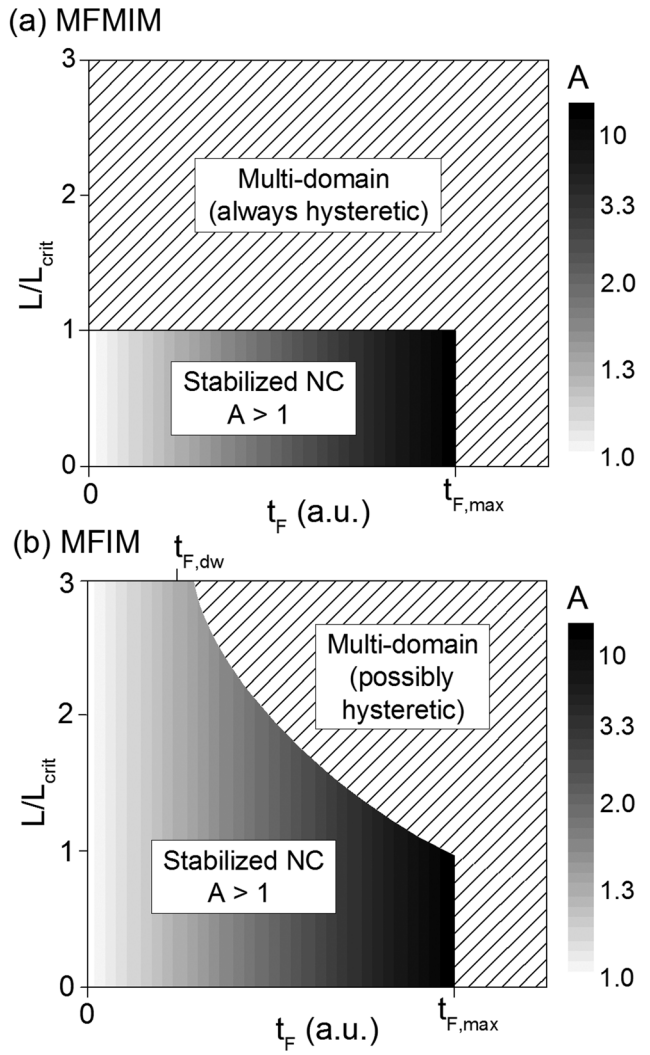

Fig. 5 Voltage amplification A and NC stabilization regime as a function of the ferroelectric thickness t_F and the lateral dimension L for (a) the MFMIM and (b) the MFIM structure.

3. Conclusion

The concept of stabilized NC in ferroelectric materials is promising for low power nanoscale device applications. However, it was shown that homogeneous single-domain Landau theory is not sufficient to correctly describe this phenomenon. When considering the background permittivity of the ferroelectric as well as domain formation, the thickness range in which the NC state is stabilized can be severely limited. Even in the single-domain case, the requirement of hysteresis-free operation is associated with a maximum critical thickness $t_{F,max}$ of the ferroelectric, which is reduced when considering the background permittivity. Furthermore, when considering domain formation, one has to distinguish the proposed structures with and without a metal layer in between the ferroelectric and the dielectric. In the case with this metal layer, NC cannot be stabilized because of anti-parallel domain formation, which can only be impeded if the lateral device dimensions are below a critical value L_{crit}, which should be in the range of nanometers for typical ferroelectrics. In the case without metal in between both layers, however, it is theoretically possible to stabilize NC even in films with large lateral dimensions. Nevertheless, the critical thickness is reduced and the maximum attainable amplification will be severely limited in this case. Reducing the lateral device dimensions towards the nanoscale is proposed to enhance the thickness range of NC stabilization as well as the maximum possible amplification in such devices. It was also shown that not the total positive capacitance of the dielectric is decisive for NC stabilization, but only the permittivity, since the electric field lines close in a certain region in proximity to the ferroelectric/dielectric interface.

In conclusion, NC devices should be designed without a metal in between the ferroelectric and the dielectric due to domain formation. To stabilize NC without this metal layer, the thickness of the ferroelectric has to be small enough so that domains cannot form, but not too thin in order to obtain sufficient amplification. Scaling such devices towards nanoscale lateral dimensions will increase the domain wall energy, thus possibly improving NC stabilization and voltage amplification.

Conflicts of interest

There are no conflicts to declare.

Final edited form was published in "Nanoscale". 2018, 10(23), S. 10891-10899. ISSN 2040-3372.
https://doi.org/10.1039/C8NR02752H

Acknowledgements

This project has received funding from the Electronic Component Systems for European Leadership Joint Undertaking under grant agreement no 692519. This Joint Undertaking receives support from the European Union's Horizon 2020 research and innovation programme and Belgium, Germany, France, Netherlands, Poland, United Kingdom. This work was also supported in part by the EFRE fund of the European Commission and in part by the Free State of Saxony (Germany).

References

1 T. N. Theis and P. M. Solomon, *Science*, 2010, **327**, 1600–1601.
2 V. V. Zhirnov and R. K. Cavin, *Nat. Nanotechnol.*, 2008, **3**, 77–78.
3 S. Salahuddin and S. Datta, *Nano Lett.*, 2008, **8**, 405–410.
4 A. I. Khan, D. Bhowmik, P. Yu, S. J. Kim, X. Pan, R. Ramesh and S. Salahuddin, *Appl. Phys. Lett.*, 2011, **99**, 113501.
5 W. Gao, A. Khan, X. Marti, C. Nelson, C. Serrao, J. Ravichandran, R. Ramesh and S. Salahuddin, *Nano Lett.*, 2014, **14**, 5814–5819.
6 D. J. R. Appleby, N. K. Ponon, K. S. K. Kwa, B. Zou, P. K. Petrov, T. Wang, N. M. Alford and A. O'Neill, *Nano Lett.*, 2014, **14**, 3864–3868.
7 A. I. Khan, K. Chatterjee, B. Wang, S. Drapcho, L. You, C. Serrao, S. R. Bakaul, R. Ramesh and S. Salahuddin, *Nat. Mater.*, 2014, **14**, 182–186.
8 M. Hoffmann, M. Pešić, K. Chatterjee, A. I. Khan, S. Salahuddin, S. Slesazeck, U. Schroeder and T. Mikolajick, *Adv. Funct. Mater.*, 2016, **26**, 8643–8649.
9 A. I. Khan, M. Hoffmann, K. Chatterjee, Z. Lu, R. Xu, C. Serrao, S. Smith, L. W. Martin, C. Hu, R. Ramesh and S. Salahuddin, *Appl. Phys. Lett.*, 2017, **111**, 253501.
10 M. Hoffmann, A. I. Khan, C. Serrao, Z. Lu, S. Salahuddin, M. Pešić, S. Slesazeck, U. Schroeder and T. Mikolajick, *J. Appl. Phys.*, 2018, **123**, 184101.
11 A. Cano and D. Jiménez, *Appl. Phys. Lett.*, 2010, **97**, 133509.
12 P. Zubko, J. C. Wojdeł, M. Hadjimichael, S. Fernandez-Pena, A. Sené, I. Luk'yanchuk, J.-M. Triscone and J. Íñiguez, *Nature*, 2016, **534**, 524–528.
13 J. L. Bjorkstam and R. E. Oettel, *Phys. Rev.*, 1967, **159**, 427–430.
14 W. Y. Shih, W.-H. Shih and I. A. Aksay, *Phys. Rev. B: Condens. Matter Mater. Phys.*, 1994, **50**, 15575–15585.
15 A. Kopal, T. Bahnik and J. Fousek, *Ferroelectrics*, 1997, **202**, 267–274.
16 A. M. Bratkovsky and A. P. Levanyuk, *Phys. Rev. Lett.*, 2000, **84**, 3177–3180.
17 G. B. Stephenson and K. R. Elder, *J. Appl. Phys.*, 2006, **100**, 051601.
18 C. H. Ahn, K. M. Rabe and J.-M. Triscone, *Science*, 2004, **303**, 488–491.
19 B.-K. Lai, I. Ponomareva, I. Kornev, L. Bellaiche and G. Salamo, *Appl. Phys. Lett.*, 2007, **91**, 152909.
20 M. Hoffmann, M. Pešić, S. Slesazeck, U. Schroeder and T. Mikolajick, 2017 Joint International EUROSOI Workshop and International Conference on Ultimate Integration on Silicon (ULIS), Athens, Greece, 2017, pp. 1–4.
21 Z. Zhu, H. Zhu, S. Wang, Y. Liu, X. Yin, K. Jia and C. Zhao, *IEEE Electron Device Lett.*, 2017, **38**, 1167–1179.
22 A. M. Bratkovsky and A. P. Levanyuk, *Phys. Rev. B: Condens. Matter Mater. Phys.*, 2001, **63**, 132103.
23 A. M. Bratkovsky and A. P. Levanyuk, *Appl. Phys. Lett.*, 2006, **89**, 253108.
24 A. L. Roytburd, S. Zhong and S. P. Alpay, *Appl. Phys. Lett.*, 2005, **87**, 092902.
25 A. Kopal, P. Mokrý, J. Fousek and T. Bahník, *Ferroelectrics*, 1999, **223**, 127–134.
26 T. Sluka, P. Mokrý and N. Setter, *Appl. Phys. Lett.*, 2017, **111**, 152902.
27 M. Kobayashi and T. Hiramoto, *AIP Adv.*, 2016, **6**, 025113.
28 K. Ng, S. J. Hillenius and A. Gruverman, *Solid State Commun.*, 2017, **265**, 12–14.
29 C. M. Krowne, S. W. Kirchoefer, W. Chang, J. M. Pond and L. M. B. Alldredge, *Nano Lett.*, 2011, **11**, 988–992.
30 C. M. Krowne, *J. Adv. Dielectr.*, 2014, **04**, 1450024.
31 K. Chatterjee, A. J. Rosner and S. Salahuddin, *IEEE Electron Device Lett.*, 2017, **38**, 1328–1330.
32 A. Rusu, G. A. Salvatore, D. Jiménez and A. M. Ionescu, Electron Devices Meeting, 2010. IEDM 2010, IEEE International, 2010, pp. 395–398.
33 D. J. Frank, P. M. Solomon, C. Dubourdieu, M. M. Frank, V. Narayanan and T. N. Theis, *IEEE Trans. Electron Devices*, 2014, **61**, 2145–2153.
34 J. Jo, W. Y. Choi, J.-D. Park, J. W. Shim, H.-Y. Yu and C. Shin, *Nano Lett.*, 2015, **15**, 4553–4556.
35 J. Jo and C. Shin, *IEEE Electron Device Lett.*, 2016, **37**, 245–248.
36 F. A. McGuire, Y.-C. Lin, K. Price, G. B. Rayner, S. Khandelwal, S. Salahuddin and A. D. Franklin, *Nano Lett.*, 2017, **17**, 4801–4806.
37 Y. J. Kim, H. Yamada, T. Moon, Y. J. Kwon, C. H. An, H. J. Kim, K. D. Kim, Y. H. Lee, S. D. Hyun, M. H. Park and C. S. Hwang, *Nano Lett.*, 2016, **16**, 4375–4381.
38 M. Dawber, C. Lichtensteiger, M. Cantoni, M. Veithen, P. Ghosez, K. Johnston, K. M. Rabe and J.-M. Triscone, *Phys. Rev. Lett.*, 2005, **95**, 177601.
39 D. A. Tenne, A. Bruchhausen, N. D. Lanzillotti-Kimura, A. Fainstein, R. S. Katiyar, A. Cantarero, A. Soukiassian, V. Vaithyanathan, J. H. Haeni, W. Tian, D. G. Schlom, K. J. Choi, D. M. Kim, C. B. Eom, H. P. Sun, X. Q. Pan, Y. L. Li, L. Q. Chen, Q. X. Jia, S. M. Nakhmanson, K. M. Rabe and X. X. Xi, *Science*, 2006, **313**, 1614–1616.
40 C. Woo and Y. Zheng, *Appl. Phys. A*, 2008, **91**, 59–63.

41 A. I. Khan, U. Radhakrishna, K. Chatterjee, S. Salahuddin and D. A. Antoniadis, *IEEE Trans. Electron Devices*, 2016, **63**, 4416–4422.
42 A. M. Bratkovsky and A. P. Levanyuk, *J. Comput. Theor. Nanosci.*, 2009, **6**, 465–489.
43 M. Lines and A. Glass, *Principles and Applications of Ferroelectrics and Related Materials*, OUP Oxford, 1977.
44 V. A. Stephanovich, I. A. Luk'yanchuk and M. G. Karkut, *Phys. Rev. Lett.*, 2005, **94**, 047601.
45 S. Kasamatsu, S. Watanabe, C. S. Hwang and S. Han, *Adv. Mater.*, 2016, **28**, 335–340.
46 J. Müller, T. S. Böscke, U. Schröder, S. Mueller, D. Bräuhaus, U. Böttger, L. Frey and T. Mikolajick, *Nano Lett.*, 2012, **12**, 4318–4323.